Available online at www.sciencedirect.com
SCIENCE DIRECT®
Journal of Chromatography A, 995 (2003) 37–54
JOURNAL OF CHROMATOGRAPHY A
www.elsevier.com/locate/chroma

Effect of the mobile phase composition on the isotherm parameters and the high concentration band profiles in reversed-phase liquid chromatography

Fabrice Gritti[a,b], Georges Guiochon[a,b,*]

[a]*Department of Chemistry, University of Tennessee, Knoxville, TN 37996-1600, USA*
[b]*Division of Chemical Sciences, Oak Ridge National Laboratory, Oak Ridge, TN, USA*

Received 29 January 2003; received in revised form 10 March 2003; accepted 11 March 2003

Abstract

Single-component adsorption isotherm data were acquired by frontal analysis for phenol on a C_{18}-Kromasil packed column, under reversed-phase liquid chromatography conditions, using various methanol–water solutions (30–60%, v/v, methanol). The isotherm model accounting best for these data was the biLangmuir model. With increasing methanol content, the two saturation capacities decrease, particularly that of the high-energy sites, the adsorption constant of the low-energy sites decreases significantly and that of the high-energy sites decreases strongly. These results allow a quantitative investigation of the properties of the high-energy sites (which are not necessarily the so-called active sites), a feature rarely discussed yet. The band profiles calculated with the numerical values of the isotherm model parameters derived by fitting the frontal analysis data to the model and using the equilibrium–dispersive model agree very well with the experimental band profiles in the whole concentration range.

Keywords: Mobile phase composition; Band profiles; Frontal analysis; Adsorption isotherms; Adsorption energy distribution; Phenol

1. Introduction

Considerable progress was made in the last 10 years in the understanding of the chromatographic process [1,2]. It has become possible to calculate the optimum design and operating conditions of a high-performance liquid chromatography (HPLC) separation [1,3]. However, these calculations require the a priori accurate understanding of the thermodynamics and the kinetics of the phase equilibrium involved in the separation studied. The former is characterized by the competitive isotherms of the feed components, the latter by the rate coefficients of the various steps involved in the mass transfers across the column [1,2]. Elution band profiles are largely controlled by phase equilibrium thermodynamics, particularly at high concentrations and when the mass transfer kinetics is not very slow [1]. The separation of feed components by reversed-phase liquid chromatography (RPLC), using C_{18}-bonded silica phases, is often optimized by adjusting the

*Corresponding author. Department of Chemistry, University of Tennessee, Knoxville, TN 37996-1600, USA. Tel.: +1-865-974-0733; fax: +1-865-974-2667.
E-mail address: guiochon@utk.edu (G. Guiochon).

0021-9673/03/$ – see front matter
doi:10.1016/S0021-9673(03)00489-8

quantity of organic solvent or modifier in the aqueous mobile phase. The control of the mobile phase composition provides a powerful means of manipulating retention and separation factors, hence to a degree, the separation of the feed components. Yet, in so doing, the separation scientist often ignores the influence of the mobile phase composition on another important parameter of the phase equilibrium, the saturation capacity of the isotherm or the amount of adsorbate needed to complete a monolayer on the adsorbent surface. It has thus become a new, interesting challenge, better to understand the effect of the mobile phase composition on the adsorption isotherm of single components.

There is ample evidence in the literature that changes of the mobile phase composition affect significantly the properties of the interfacial region at the C_{18}-bonded silica surface [4–9]. For example, variations of the column hold-up volume [7,8] or nuclear magnetic resonance (NMR) measurements of the relaxation times of labeled molecules of organic modifiers [4–6] have experimentally demonstrated the importance of this effect. It is likely that any phenomenon leading to a significant modification of the adsorption energy of the sample components at the liquid–solid interface will also cause changes in the monolayer capacity. This, in turn, will greatly affect the elution band profiles under nonlinear conditions. The explanation for that is mainly twofold: (i) the addition of an organic solvent to the aqueous mobile phase induces to a degree the competition for adsorption between the sample components and this organic modifier; and (ii), as a result of the preferential adsorption of the modifier and of the presence of residual accessible silanols, the structure of the C_{18} chains that define the interphase between the mobile phase and the solid silica will be affected. A low organic modifier content causes the collapse of the bonded chains that are brought together by the intermolecular C_{18} dispersive interactions while they tend to exclude water. A high organic modifier content induces the rupture of the C_{18} intermolecular interactions via chain solvation by the modifier and the formation of a ‘‘brush-like’’ structure. Some authors have quantified this preferential adsorption of organic solvents by measuring the isotherms of methanol (MeOH), acetonitrile (ACN) and tetrahydrofuran (THF) on C_{18}-silica from pure water [9] and they showed how crucial was the role of these mobile phase modifiers on the resulting column hold-up volume.

Another popular explanation stems from the effect of large sample concentrations that are frequently used in preparative liquid chromatography. High feed component concentrations change the polarity of the mobile phase in contact with the stationary phase, perturbing the interfacial boundary between the stationary and the mobile phases. This may complicate the modeling of the adsorption isotherm.

Only little and usually anecdotal information is available in the literature on the influence of the mobile phase composition on any other parameters of the isotherm than its initial slope (i.e., the limit retention factor at zero solute concentration). The dependence of the monolayer saturation capacity and of the possible other binding constants on the composition of the mobile phase has rarely been investigated systematically [10]. Jandera and Guiochon [11] have studied the effect of the sample solvent on the band profiles of poorly soluble feed components in preparative chromatography and showed the need to account for the dependence of the isotherm coefficients on the mobile phase composition when implementing the classical models of chromatography to calculate band profiles. El Fallah and Guiochon [12] studied the band profiles of large samples of 2-phenylethanol under nonlinear conditions in gradient elution but did not need to consider the dependence of the saturation capacity on the concentration of the organic modifier because acetonitrile was used and the problem was treated as a competitive problem. This is not the case with methanol, however, and there seem to be no general results on the influence of the nature and concentration of methanol, the simplest organic modifier, on the saturation capacity of even simple compounds. Yet, this parameter determines the loading factor obtained when injecting a given sample size into a column, hence the production rate that can be achieved with a particular combination of stationary and mobile phase.

The goal of this work was to determine the effect of the nature and composition of the mobile phase on the adsorption isotherm and the band profiles of a small polar compound, phenol. We investigated its equilibrium isotherm on a C_{18}-silica (Kromasil)

column, using aqueous mobile phases modified by different concentrations of methanol. We showed in a previous paper [13] that the adsorption isotherm of phenol on this stationary phase, in the phenol concentration range 0–30 g/l, was modeled by a biLangmuir isotherm. Thus, this system is also a useful tool for a quantitative study of the influence of high-energy sites, having a low saturation capacity, on the adsorption of polar samples. In this work, we study the effect of the composition of methanol–water solutions on the parameters of the biLangmuir isotherm model, measured by frontal analysis, in two concentration ranges, 0–50 and 0–100 g/l. In a forthcoming publication, we will investigate the effects of the nature and concentration of other organic modifiers (ACN, isopropanol, and THF) on the adsorption of phenol.

2. Theory

2.1. Determination of single-component isotherms by frontal analysis

Frontal analysis (FA) was used to determine the single-component isotherm data needed in this work because it is the most accurate method [1–3]. It consists in the successive replacement of the stream of mobile phase percolating through the column with streams of solutions of the studied compound of increasing concentrations, in the recording of the breakthrough curves at the column outlet, and in the washing of the column with pure mobile phase before undertaking the next step. Mass conservation of the solute between the times when the new solution enters the column and when the plateau concentration is reached allows the calculation of the adsorbed amount, q^*, of solute in the stationary phase at equilibrium with a given mobile phase concentration, C. This amount is best measured by integrating the breakthrough curve (equal area method) [14]. The adsorbed amount q^* is given by:

$$q^* = \frac{C(V_{eq} - V_0)}{V_a} \quad (1)$$

where V_{eq} and V_0 are the elution volume of the equivalent area of the solute and the hold-up volume, respectively, and V_a is the volume of stationary phase.

2.2. Models of single-component isotherm

2.2.1. The Langmuir isotherm

This model is the most frequently used in general studies of liquid–solid chromatographic equilibria, in spite of its semi-empirical nature [15,16]. It is written:

$$q^* = q_S \cdot \frac{bC}{1 + bC} \quad (2)$$

In this model, q_S is the monolayer saturation capacity of the adsorbent and b is the equilibrium constant of adsorption. This model assumes that the surface of the adsorbent is homogeneous, that adsorption is localized, and that there are no adsorbate–adsorbate interactions. The equilibrium constant b is given by the following equation [17]:

$$b = b_0 e^{\frac{\varepsilon_a}{RT}} \quad (3)$$

where ε_a is the energy of adsorption, R is the universal ideal gas constant, T the absolute temperature and b_0 is a preexponential factor that could be derived from the molecular partition functions in both the bulk and the adsorbed phases. Consistent with the basic assumption of this model, the affinity energy distribution (AED), $F(\varepsilon)$, corresponding to the Langmuir isotherm is a Dirac function:

$$F(\varepsilon) = \delta(\varepsilon - \varepsilon_a) \quad (4)$$

The surface is homogeneous, hence has a unimodal energy distribution with a mode width equal to 0.

2.2.2. The biLangmuir isotherm

This model is the simplest one for a nonhomogeneous surface [18]. The surface is assumed to be paved with two different types of homogeneous chemical domains which behave independently. Then, the equilibrium isotherm results from the addition of two independent local Langmuir isotherms:

$$q^* = q_{S,1} \cdot \frac{b_1 C}{1 + b_1 C} + q_{S,2} \cdot \frac{b_2 C}{1 + b_2 C} \quad (5)$$

In this model, there are two saturation capacities, $q_{S,1}$ and $q_{S,2}$, corresponding to each one of the two types of sites. The two equilibrium constants b_1 and b_2 are associated with the adsorption energies $\varepsilon_{a,1}$ and $\varepsilon_{a,2}$, through Eq. (3). The AED becomes:

$$F(\varepsilon) = \frac{q_{S,1}}{q_S} \cdot \delta(\varepsilon - \varepsilon_{a,1}) + \frac{q_{S,2}}{q_S} \cdot \delta(\varepsilon - \varepsilon_{a,2}) \quad (6)$$

This is a bimodal energy distribution and both modes have a width 0.

2.3. Calculation of the affinity energy distributions

Actual surfaces are not homogeneous, as was assumed so far. These surfaces are characterized by an AED. The experimental isotherm on such a surface is the sum of the isotherms on each one of the homogeneous fractions of the surface, fractions that correspond to given energies of the AED. Under the condition of a continuous distribution and assuming a Langmuir local isotherm model, this sum can be replaced by an integral and the overall adsorption isotherm can be written [17]:

$$q^*(C) = \int_0^\infty F(\varepsilon) \cdot \frac{b(\varepsilon)C}{[1 + b(\varepsilon)C]} \cdot d\varepsilon \quad (7)$$

where $q^*(C)$ is the total amount of solute adsorbed on the surface at equilibrium with a concentration C, ε is the binding energy between an adsorbed solute molecule and the surface of the adsorbent, b is the associated binding constant and is related to ε though Eq. (3).

The normalization condition for the AED is:

$$\int_0^\infty F(\varepsilon) d\varepsilon = q_S \quad (8)$$

where q_S is the overall saturation capacity.

To characterize the behavior of a heterogeneous surface, the AED, $F(\varepsilon)$, is derived from the isotherm data, a procedure for which there is a variety of methods [17,19–21]. Most of them either use a preliminary smoothing of the experimental data and fit the smoothed data to an isotherm model or search for an AED given by a certain function. In this work, the expectation–maximization (EM) method [21] was used. It is a computer-intensive method that uses directly the raw experimental data (M data points), without injecting any arbitrary information into the derivation. The distribution function $F(\varepsilon)$ is discretized using an N-grid points in the energy space (i.e., assuming that the surface is made of a set of N homogeneous surfaces) and the corresponding values of $F(\varepsilon)$ are estimated from the data points. The energy space is limited by ε_{min} and ε_{max}. These energy boundaries are obtained from the maximum and minimum concentrations applied in FA, by using Eq. (3) (with $b_{min} = 1/C_{max}$, $b_{max} = 1/C_{min}$) but a narrower range may be considered as long as it accommodates the data. The amount $q(C_i)$ of solute adsorbed at concentration C_j is iteratively estimated by:

$$q^k_{cal}(C_j) = \sum_{\varepsilon_{min}}^{\varepsilon_{max}} F^k(\varepsilon_i) \cdot \frac{b(\varepsilon_i) C_j}{[1 + b(\varepsilon_i) C_j]} \cdot \Delta\varepsilon$$
$$j \in [1,M];\ i \in [1,N] \quad (9)$$

with:

$$\Delta\varepsilon = \frac{\varepsilon_{max} - \varepsilon_{min}}{N - 1} \qquad \varepsilon_i = \varepsilon_{min} + (i - 1) \cdot \Delta\varepsilon \quad (10)$$

The index k indicates the kth iteration of the numerical calculation of the AED function. The initial guess (iteration $k = 0$) of the AED function $F(\varepsilon_i)$ is the uniform distribution (over the N fictitious adsorption sites) of the maximum adsorbed amount observed experimentally. This initial guess has the advantage of introducing the minimum bias into the AED calculation.

$$F^0(\varepsilon_i) = \frac{q(C_M)}{N} \quad \forall i \in [1,N] \quad (11)$$

Actually, the EM program calculates the amount adsorbed by taking $b(\varepsilon_i)$ as the variable in the energy space, so that neither the temperature nor the pre-exponential factor need to be defined. Only M, N, b_{min}, b_{max} and the number of iterations must be defined to start the calculation. b_{min} and b_{max} are related to the reciprocal of the highest and the lowest concentration applied in FA, respectively. It is noteworthy that, to obtain any information on the adsorption energy, an assumption must be made for b_0 in Eq. (3). The final result is the distribution of the equilibrium constants. In this work, the AEDs are

plots of the discretized variable $q_{S,i}$, the saturation capacity of the sites the energy of which belongs to the interval $[\varepsilon_i, \varepsilon_i + \Delta\varepsilon]$ (see Eq. (3)), versus ln (b_i).

The distribution function is updated after each iteration by:

$$F^{k+1}(\varepsilon_i) = F^k(\varepsilon_i) \sum_{c_{min}}^{c_{max}} \frac{b(\varepsilon_i)\, C}{[1 + b(\varepsilon_i)\, C]} \cdot \Delta\varepsilon \cdot \frac{q_{exp}(C_j)}{q^k_{cal}(C_j)} \tag{12}$$

The EM procedure protects better than most other methods against the consequences of the possible incorporation of experimental artifacts into the calculation of AED or against the effect of modeling the experimental data (and particularly the noise and drift that the data may contain).

2.4. Modeling of band profiles in HPLC

The profiles of overloaded elution bands were calculated, using the isotherm determined by FA and the equilibrium–dispersive model (ED) of chromatography, under the same experimental conditions as those used to record the chromatograms of large samples [1,22,23]. The ED model assumes instantaneous equilibrium between mobile and stationary phases and a finite column efficiency originating from an apparent axial dispersion coefficient, D_a, that accounts for the dispersive phenomena (molecular and eddy diffusion) and for the non-equilibrium effects that take place in a chromatographic column. The axial dispersion coefficient is:

$$D_a = \frac{uL}{2N} \tag{13}$$

where u is the mobile phase linear velocity, L the column length, and N the number of theoretical plates or apparent efficiency of the column, measured under linear conditions, i.e., with a small sample size.

In this model, the mass balance equation for a single component is expressed as follows:

$$\frac{\partial C}{\partial t} + u \cdot \frac{\partial C}{\partial z} + F \cdot \frac{\partial q^*}{\partial t} - D_a \cdot \frac{\partial^2 C}{\partial z^2} = 0 \tag{14}$$

where q^* and C are the stationary and mobile phase concentrations of the adsorbate, respectively, t is the time, z the distance along the column, and $F = (1 - \varepsilon_t)/\varepsilon_t$ is the phase ratio at the solute concentration, with ε_t the total column porosity (F is a function of the solute concentration in the present study). q^* is related to C through the isotherm equation, $q^* = f(C)$.

2.4.1. Initial and boundary conditions for the ED model

At $t = 0$, the concentrations of the solute and adsorbate in the column are uniformly equal to zero, and the stationary phase is in equilibrium with the pure mobile phase. The boundary conditions used are the classical Danckwerts-type boundary conditions [1,24] at the inlet and outlet of the column.

2.4.2. Numerical solutions of the ED model

The ED model was solved using a computer program based on an implementation of the method of orthogonal collocation on finite elements (OCFE) [25–27]. The set of discretized ordinary differential equations was solved with the Adams–Moulton method, implemented in the VODE procedure [28]. The relative and absolute errors of the numerical calculations were $1 \cdot 10^{-6}$ and $1 \cdot 10^{-8}$, respectively.

3. Experimental

3.1. Chemicals

The mobile phase used in this work was a mixture of HPLC-grade water and HPLC-grade methanol, both purchased from Fisher Scientific (Fair Lawn, NJ, USA). The same mobile phases were used for the determination of the single-component adsorption isotherm data and for the recording of a large size band profile of the pure compound (phenol). The solvents used to prepare the mobile phase were filtered before use on an SFCA (surfactant free cellulose acetate) filter membrane, 0.2 μm pore size (Suwannee, GA, USA).

The solutes used were uracil and phenol. Both were obtained from Aldrich (Milwaukee, WI, USA).

3.2. Materials

A manufacturer-packed, 250×4.6 mm Kromasil

column was used (column E6021, Eka Nobel, Bohus, Sweden). This column was packed with a C_{18}-bonded, endcapped, porous silica. It was one of the lot of 10 columns (columns E6019, E6103–E6106, E6021–E6024 and E6436) previously used by Kele and Guiochon [29] and Gritti and Guiochon [30] for their studies of the reproducibility of the chromatographic properties of RPLC columns under linear [28] and non-linear [29] conditions, respectively. The main characteristics of the bare porous silica and of the packing material used are summarized in Table 1.

The hold-up time of this column was derived from the retention time of uracil injections. Whatever the mobile phase used, the elution time of uracil is nearly the same as that of methanol or sodium nitrate. The product of this time and the mobile phase flow-rate gives an excellent estimate of the column void volume. Plots of the void volume of the column versus the mobile phase composition recorded at the beginning and the end of the experimental measurements reported in this work are shown in Fig. 1.

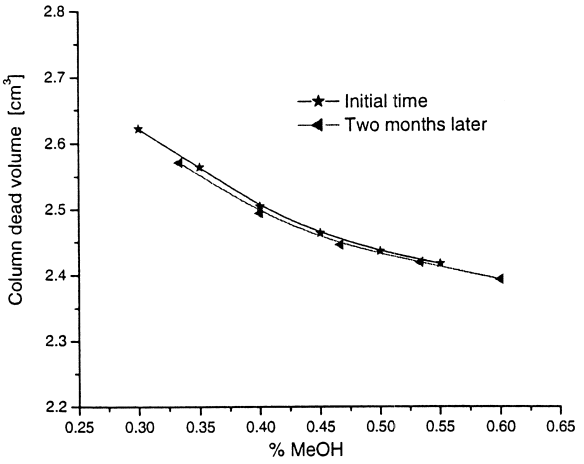

Fig. 1. Hold-up volume of the C_{18}-Kromasil column as a function of the composition of the mobile phase for two different series of measurements.

3.3. Apparatus

The isotherm data were acquired using a Hewlett-Packard (Palo Alto, CA, USA) HP 1090 liquid chromatograph. This instrument includes a multi-solvent delivery system (tank volumes, 1 dm^3 each), an auto-sampler with a 25 μl sample loop, a diode-array UV detector, a column thermostat and a computer data acquisition station. Compressed nitrogen and helium bottles (National Welders, Charlotte, NC, USA) are connected to the instrument to allow the continuous operations of the pump, the auto-sampler, and the solvent sparging. The extra-column volumes are 0.068 and 0.90 ml as measured from the auto-sampler and from the pump system, respectively, to the column inlet. All the retention data were corrected for this contribution. The flow-rate accuracy was controlled by pumping the pure mobile phase at 23 °C and 1 ml/min during 50 min, from each pump head, successively, into a volumetric glass of 50 ml. A relative error of less than 0.4% was obtained so that we can estimate the long-term accuracy of the flow-rate at 4 μl/min at flow-rates around 1 ml/min. All measurements were carried out at a constant temperature of 23 °C, fixed by the laboratory air-conditioner. The daily variation of the ambient temperature never exceeded ±1 °C.

Table 1
Physico-chemical properties of the packed Kromasil-C_{18} (Eka) E6021 column

Particle size	5.98 μm
Particle size distribution (90:10, % ratio)	1.44
Pore size	112 Å
Pore volume	0.88 ml/g
Surface area	314 m^2/g
Na, Al, Fe content	11; <10; <10 ppm
Particle shape	Spherical
Total carbon	20.00%
Surface coverage	3.59 μmol/m^2
Endcapping	Yes

3.4. Isotherm measurements by frontal analysis

The range of compositions of the methanol–water solutions used as the mobile phase for single-component FA measurements must be chosen according to the retention factor of the solute at infinite dilution. In order to acquire a sufficient number of data points and to achieve measurements of a satisfactory accuracy, the retention factor should be

neither too high nor too low. Values between 1 and 5 are most convenient. Hence, a range of methanol–water compositions from 30:70 to 60:30 was selected for this work. Prior to the isotherm determinations, approximate values of the solubilities of phenol in solutions of this composition range, at 23 °C, were determined by stepwise additions of 0.5 ml of the pure mobile phase into a volume of 25 ml of a saturated solution, until complete dissolution. Accordingly, FA measurements can be carried out at phenol concentrations of up to 100 g/l. Two series of FA experiments were conducted successively, with different maximum concentrations applied. First, 30 consecutive breakthrough curves were recorded with a maximum concentration of 50 g/l of phenol, at methanol concentrations of 30, 35, 40, 45, 50 and 55% in the mobile phase. Two months later, a series of 15 consecutive breakthrough curves were recorded with a maximum concentration of 100 g/l of phenol, for methanol concentrations of 33.3, 40, 46.7, 53.3 and 60%. The comparison of the results of these two independent series allows the assessment of the reproducibility of the adsorption data and the validation of the evolution of the isotherm parameters with the methanol concentration.

One pump of the HPLC instrument was used to deliver a stream of the pure mobile phase, the second pump a stream of the pure sample solution. The concentration of the studied compound in the FA stream is determined by the concentration of the mother sample solution and the flow-rate fractions delivered by the two pumps. The breakthrough curves are recorded successively at a flow-rate of 1 ml/min, with a sufficiently long time delay between each breakthrough curve to allow for the reequilibration of the column with the pure mobile phase. The injection time of the sample was fixed at 5 min for all FA steps in order to reach a stable plateau at the column outlet. To avoid recording any UV-absorbance signal larger than 1500 mAU and the corresponding signal noise, the detector signal was detected at 292 nm for all mobile phases. The detector response for phenol was calibrated accordingly.

The overloaded profile needed for the validation of the fitted isotherms was recorded for each mobile phase composition, during the frontal analysis sequence.

4. Results and discussion

4.1. Effect of the mobile phase on the column dead volume

Fig. 1 describes the progressive change of the column volume accessible to uracil with increasing organic modifier content of the mobile phases used in this work. The reproducibility of these results over a 2-month period is excellent. A relative variation of less than 0.7% is observed between the two series of measurements. The total pore volume increases with decreasing methanol concentration. This observation is not new [7,8]. It merely confirms how much the degree of swelling of the C_{18} chains may significantly depend on the nature and the amount of the organic solvent present in the mobile phase. This swelling is a direct consequence of the intermolecular interactions between the solvent, the C_{18} chains, and the accessible siloxanes and residual silanols on the silica surface. There is a simple correlation between the swelling of the chains observed and the increasing energy of the dispersion interactions, i.e., with increasing methanol concentration. In other words, the amount of organic solvent embedded within the layer of C_{18} chains bonded to the silica surface increases with this concentration.

To summarize, the structure of the C_{18} chains, their degree of solvation, and their layer environment depend on the nature and the concentration of the organic solvent present in the mobile phase. According to our results, the degree of solvation of the C_{18} chains increases with increasing concentration of the organic solvent. As a result, the equilibrium isotherm of most sample solutes between the mobile and the stationary phases is also influenced by the composition of the mobile phase. We discuss now the effect of the methanol concentration of methanol–water mixtures on the adsorption isotherm of phenol.

4.2. Selection of phenol for the study of the effect of the mobile phase composition on the adsorption properties of the C_{18}-Kromasil column

Phenol was selected for this investigation for two important reasons. First, phenol is highly soluble in methanol–water mixtures. Concentrations of at least 100 g/l could easily be dissolved in all the aqueous

solutions of methanol used in this work. This allowed the achievement of adsorption measurements at high surface coverages, corresponding to solid-phase concentrations reasonably close to the column monolayer capacity. Hence, this permits the accurate determination of the isotherm parameters. As shown later, this possibility is important in order to obtain well resolved energy bands in the AED. Second, phenol is an appropriate probe to study the surface heterogeneity of the stationary phase. It was demonstrated previously [13] that its adsorption isotherm on the same packing material as the one used in this work (column E6019) is well modeled by a biLangmuir isotherm. The main argument was that the direct calculation of the AED from the raw experimental adsorption data revealed that there are two, well resolved energy bands. The low-energy sites are the most numerous and correspond probably to the locations between the C_{18} chains, i.e., to the nonselective dispersive interactions taking place in the bonded alkyl layer. The high-energy sites correspond probably to accessible residual silanols or to siloxanes exposed at the silica surface and with which phenol can undergo specific electrostatic, hydrogen-bond, or polar interactions.

The parameters of the biLangmuir isotherm (saturation capacities $q_{S,1}$ and $q_{S,2}$, binding constants b_1 and b_2) were measured in the whole range of methanol concentrations in the mobile phases used in this study. The results of these measurements and the trends in the variations of these parameters are now discussed.

4.3. Determination of the best biLangmuir isotherm parameters by isotherm fitting

Thirty adsorption data points were acquired during each FA run in the first series. Six different aqueous mobile phase compositions were investigated (methanol concentration, %, v/v: 30, 35, 40, 45, 50 and 55). The Scatchard plots shown in Fig. 2A confirms that the simple Langmuir model is inadequate to model the data since these plots are all convex downward, not the straight lines corresponding to Langmuirian behavior. A second series of data was acquired later (methanol concentration, %, v/v: 33.3, 40, 46.7, 53.3 and 60). Fig. 2B shows the consistency and the high reproducibility between

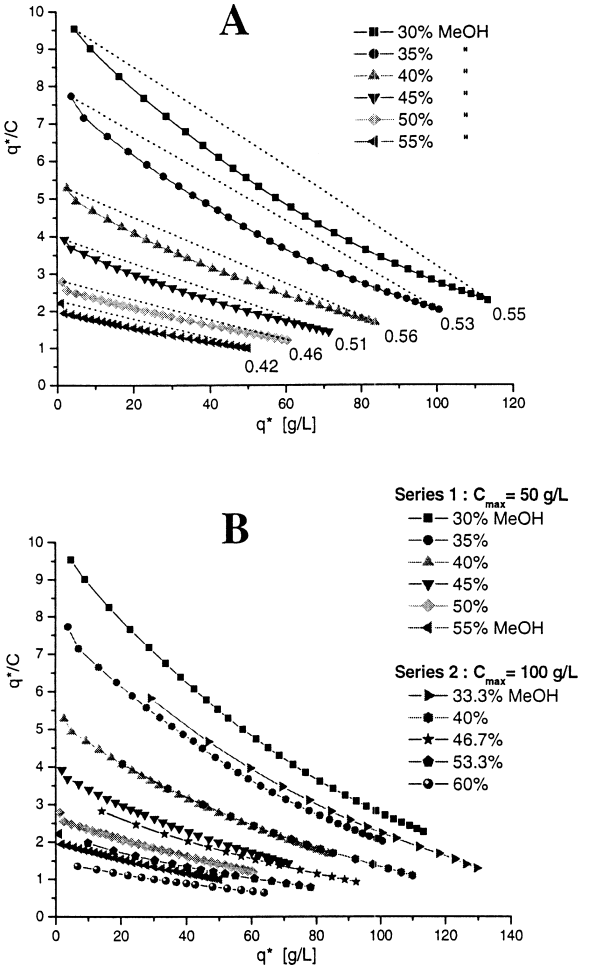

Fig. 2. Scatchard plots for the adsorption of phenol on C_{18}-Kromasil with 10 different methanol–water mobile phase compositions. (A) The maximum phenol concentration in the mobile phase is 50 g/l. (B) The maximum phenol concentration in the mobile phase is 100 g/l. Note the convex downward shape of the Scatchard plots, suggesting biLangmuirian behavior. (a) The number in the lower right corner of each curve corresponds to the ratio between the maximum adsorbed concentration at 50 g/l and the total saturation capacity derived from the best biLangmuir isotherm parameters. $T = 295$ K. (b) Note the consistency of the two series of results.

the Scatchard plots of the data acquired in the two series of FA runs. The validity of the biLangmuir model is further supported by the excellent agreement between the calculated and experimental band profiles reported in Fig. 3. The experimental adsorption data (symbols) and the curves resulting from

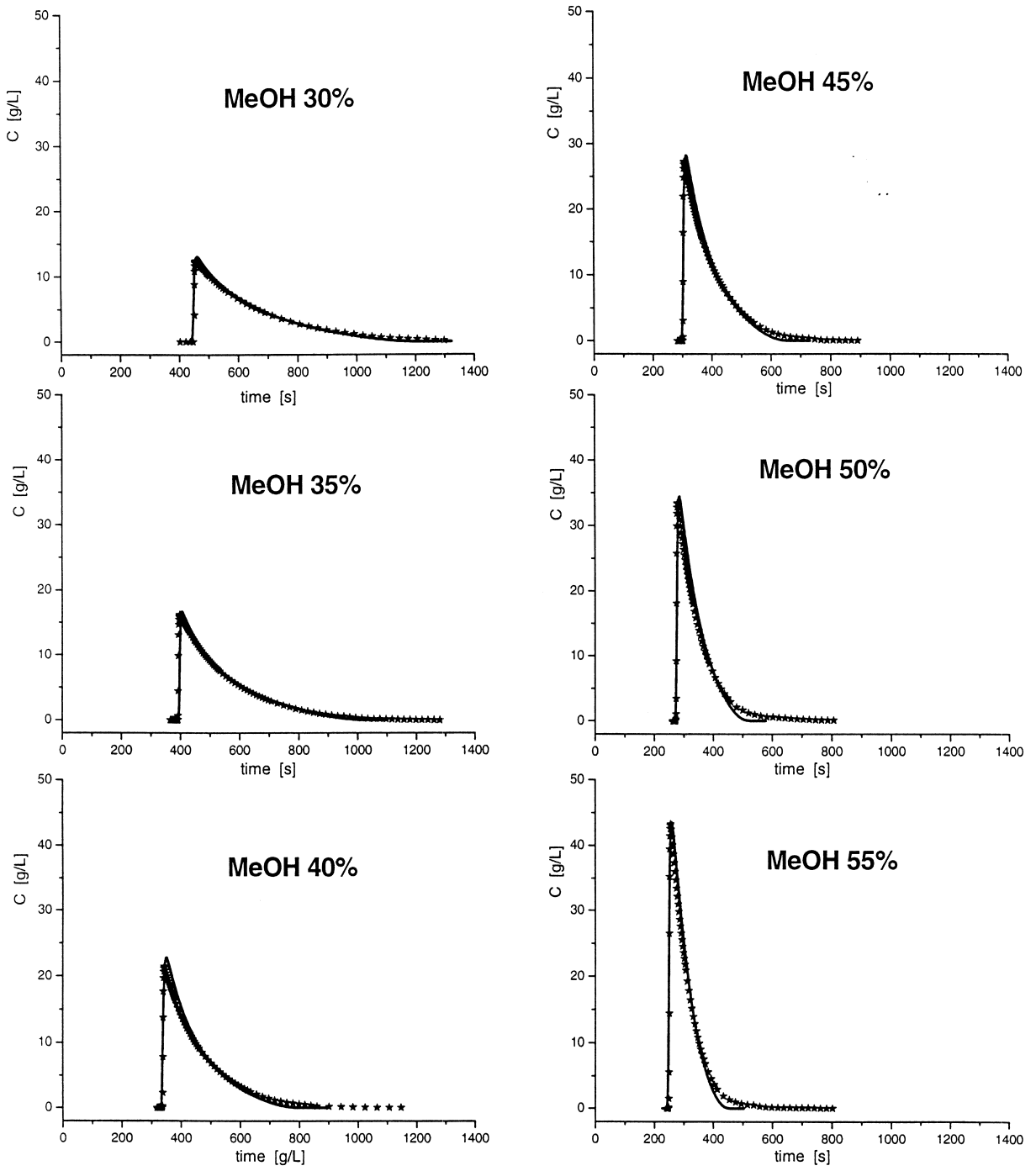

Fig. 3. Comparison between calculated (solid line) and experimental (symbols) band profiles of phenol on the Kromasil-C_{18} column with the six methanol–water mixtures as the mobile phases. Injection of a solution of phenol at 50 g/l during 60 s, $L_f \approx 15\%$. Note the very good agreement for all the mobile phases and the evolution of the shape of the band profile when methanol content increases in the mobile phase. Flow-rate 1 ml/min, $T = 295$ K. The calculations performed with the equilibrium–dispersive model used a plate number of 1000 at all methanol concentrations.

the best fits of the six sets of experimental data to the biLangmuir model are compared in Fig. 4A. The excellent reproducibility of the data for a methanol concentration of 40% is illustrated in Fig. 4B. The Fisher numbers are high, between 450 000 and 1 030 000, indicating an excellent fit. The best values derived for the saturation capacities and the binding constants are plotted in Fig. 5A and B (first data series) and in Fig. 5C and D (second data series) as functions of the mobile phase composition.

A few salient facts emerge clearly from the results of the first series of FA runs, (i) the saturation capacities of the two types of sites decrease monotonously with increasing methanol concentration in the mobile phase; (ii) the adsorption constant of the low-energy sites is nearly independent of this concentration; and (iii) the adsorption constant of the high-energy sites decreases rapidly with increasing methanol concentration. The difference in the behavior of the two types of sites is striking. When the methanol concentration in the mobile phase increases from 30 to 55%, $q_{S,1}$ decreases by only about 20% of its initial value (Fig. 5A) while, by contrast, $q_{S,2}$ loses 80% of its initial value (Fig. 5A). Similarly, the equilibrium constant b_1 of phenol on the low-energy sites remains nearly constant for methanol concentrations between 30 and 55% while b_2 decreases from 0.118 to 0.053 l/g (Fig. 5B). Therefore, we must keep in mind in the discussion of the variations of the four parameters of the biLangmuir isotherm that, although the two terms in Eq. (5) give contributions to the retention factor at infinite dilution that are of the same order of magnitude, their dependence on the methanol concentration are markedly different. From Eq. (5), we derive:

$$k_0' = F \cdot \left(\frac{dq}{dC}\right)_{c=0} = F(b_1 q_{S,1} + b_2 q_{S,2}) \qquad (15)$$

When the methanol concentration increases from 30 to 55%, the first contribution to the retention factor decreases from 1.09 to 0.92, i.e., by 15%, while the second decreases from 4.59 to 0.51, i.e., by almost a factor of 9.

It is probably correct to assimilate the low-energy type of sites to those sites with which the phenol molecules have only weak, nonpolar interactions, that involve only the bonded alkyl chains. Similarly, the high-energy type of sites includes essentially those sites with which the phenol molecules undertake stronger, polar interactions. It must be understood, however, that the sites that are considered here as high-energy sites are by no means similar to those that are conventionally referred to in chromatography as active sites and on which peak tailing is usually blamed. The total saturation capacity of the high-energy sites identified here is too large a fraction of that of the low-energy sites for these high-energy sites to be considered as the ''active'' sites. More probably, these high-energy sites include the fraction

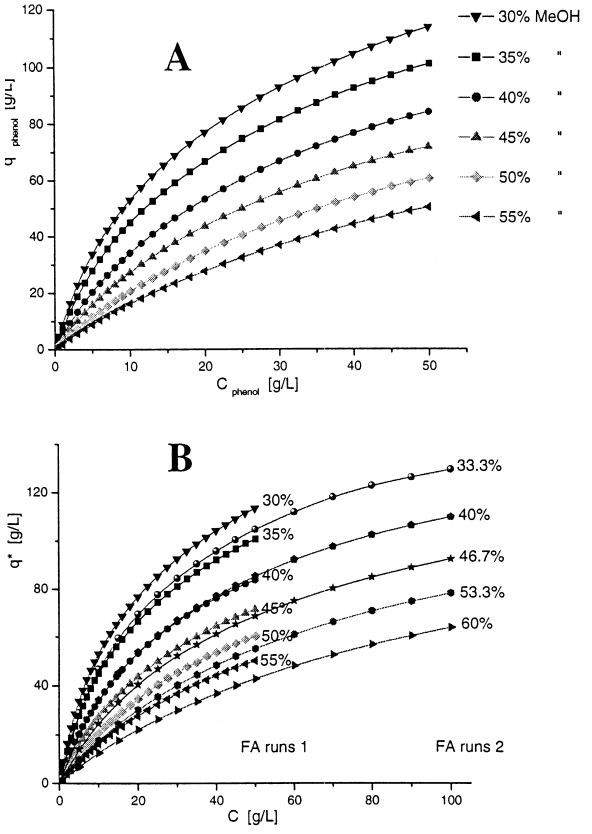

Fig. 4. Experimental isotherm data (symbols) of phenol on the packed Kromasil-C_{18} column obtained with 10 different methanol–water mixtures as the mobile phases. (a) Maximum concentration of phenol in the mobile phase, 50 g/l. (b) Maximum concentration of phenol in the mobile phase, 100 g/l. The solid line is the best fitting isotherm using the biLangmuir model. $T = 295$ K. Note the evolution of the isotherm curvature from low to high methanol content in the mobile phase and the consistency between the two series of FA runs, as well.

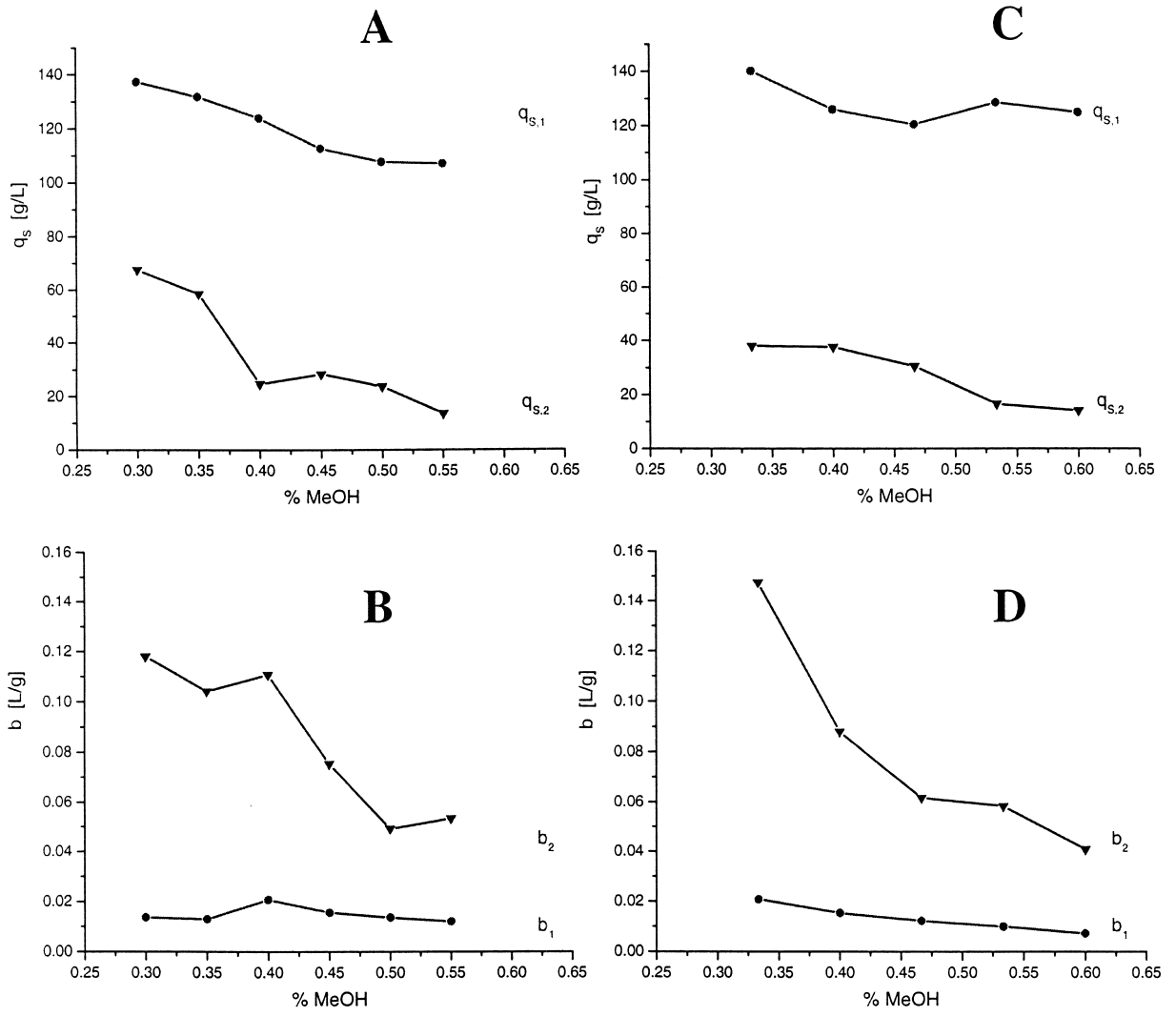

Fig. 5. Results of the regression analysis of the experimental adsorption data of phenol to the biLangmuir isotherm model for the first (left, A and B, $C_{max}=50$ g/l) and second (right, C and D, $C_{max}=100$ g/l) series of FA runs. Top (A and C), saturation capacities of the low (circle) and high (down triangle) energy sites. Bottom (B and D), adsorption constants of the low (circle) and high (down triangle) energy sites.

of the silica surface above which the density of the bonded alkyl chains is low. There, the phenol molecules can easily penetrate the alkyl layer and interact more strongly with the silica surface.

With these assumptions, the small decrease of $q_{S,1}$ with increasing methanol concentration might be explained by the weak interactions between the bonded alkyl chains and the methanol molecules. In RPLC, there is little competition for adsorption between solvent and solute molecules. The main effect of an increase in methanol concentration seems to be related to the swelling of the bonded layer of alkyl chains which still depends on the concentration in the range used here (Fig. 1). The increased concentration of methanol causes a better solvation of the C_{18} chains, hence a larger accessible surface area of contact between phenol molecules and C_{18} chains, leading to an increase of $q_{S,1}$.

However, in the same time, both the solubility of methanol in the bonded layer and the solubility of phenol in the mobile phase increase. The balance of these effects is the slight decrease of $q_{S,1}$ observed. On the other hand, the important decrease of $q_{S,2}$ can be interpreted as the result of a competition between phenol and methanol for access to these sites.

The adsorption constant b_1 of phenol on the low-energy sites remains nearly constant for methanol concentrations between 30 and 55% (Fig. 5B). As noted above, the large decrease observed for the retention factor of phenol is mostly caused by the decrease of the constant b_2. The reason for the decrease of the retention factor of phenol is in part due to the increase of its solubility in the mobile phase. The partition of phenol between the C_{18} chains and the methanol–water liquid phase is likely to be poorly dependent on the methanol content in this composition range. The reason is the same as this argued above: a higher contact area with the C_{18} chains and a more favorable phenol solvation in the mobile phase compensate each other. The decrease in the adsorption constant b_2 is probably due to the competition of methanol for interactions with the polar areas on the adsorbent surface.

These results are confirmed by those of the second series of isotherm measurements at 33.3, 40, 46.7, 53.3 and 60% methanol in the mobile phase, with a maximum concentration of 100 g/l instead of 50 g/l. The trends followed by the biLangmuir parameters is the same as the one initially observed (Fig. 5C and D). It confirms, with higher accuracy data, the trends of the adsorption constants b_1 and b_2, which appear more clearly, both to decrease monotonously with increasing methanol concentration (see Fig. 5B and D).

To summarize, the study of the adsorption isotherms of phenol shows that the retention mechanism is more complex than usually assumed on the view of results obtained under linear conditions. Our results suggest that there is a population of unidentified retention sites that may play an important role in the retention of low-molecular-mass compounds in RPLC, even on a C_{18}-endcapped stationary phase. The mobile phase composition affects only little the hydrophobic interactions between the solute and the peripheral bonded alkyl chains in the range of concentrations involved in this study. However, this composition affects strongly the adsorption constant of the solute on the high energy sites. These conclusions are derived from the results of the nonlinear regression of the adsorption data to the biLangmuir model. The choice of an isotherm model is arbitrary and could affect the conclusions of the exercise. As shown previously, there is another, independent method of interpretation of the isotherm data which consists in calculating the AED. The results of this method are independent of the choice of an isotherm model to account for the adsorption behavior of the solute.

4.4. Determination of the best isotherm parameters from the AED analysis

The calculation of the AED was done using the EM method. In all cases, the same range of energy, i.e., of b values, see Eq. (3) ($0.0005\ \mathrm{l/g} < b < 3\ \mathrm{l/g}$) and the same number of energy points ($N = 150$) were considered. For the corresponding retention factor range, between 1 and 5, this energy range largely covers the classical physisorption energies, from those of the weak dispersive interactions to those of strong, specific hydrogen-bond interactions. Four energy distribution functions were calculated for each mobile phase composition, depending on the number of iterations made in applying the EM procedure: 10^5, 10^6, 10^7 and 10^8 iterations were successively used in the program.

The results are presented in Fig. 6 and Fig. 7 that corresponds to the first and the second series of FA measurements, respectively. Concerning the first series of FA runs, the EM method converges clearly toward a bi-modal energy distribution for methanol concentrations between 30 and 45%, as expected from previous results [13] (Fig. 6). At higher methanol concentrations (50 and 55%), the AED is also bimodal but the low-energy mode could not be completely determined, for the lack of isotherm data at sufficiently high concentrations (at $C_{max} = 50$ g/l, the surface coverage, q^*/q is only 0.46 at 50% methanol while it exceeds 0.50 at 45% methanol and below). Probably for the same reason, the total saturation capacities estimated by the program at the two highest methanol concentrations are inconsistent with those derived for the four lowest concentrations, e.g., more than 300 g/l at 50 and 55% methanol

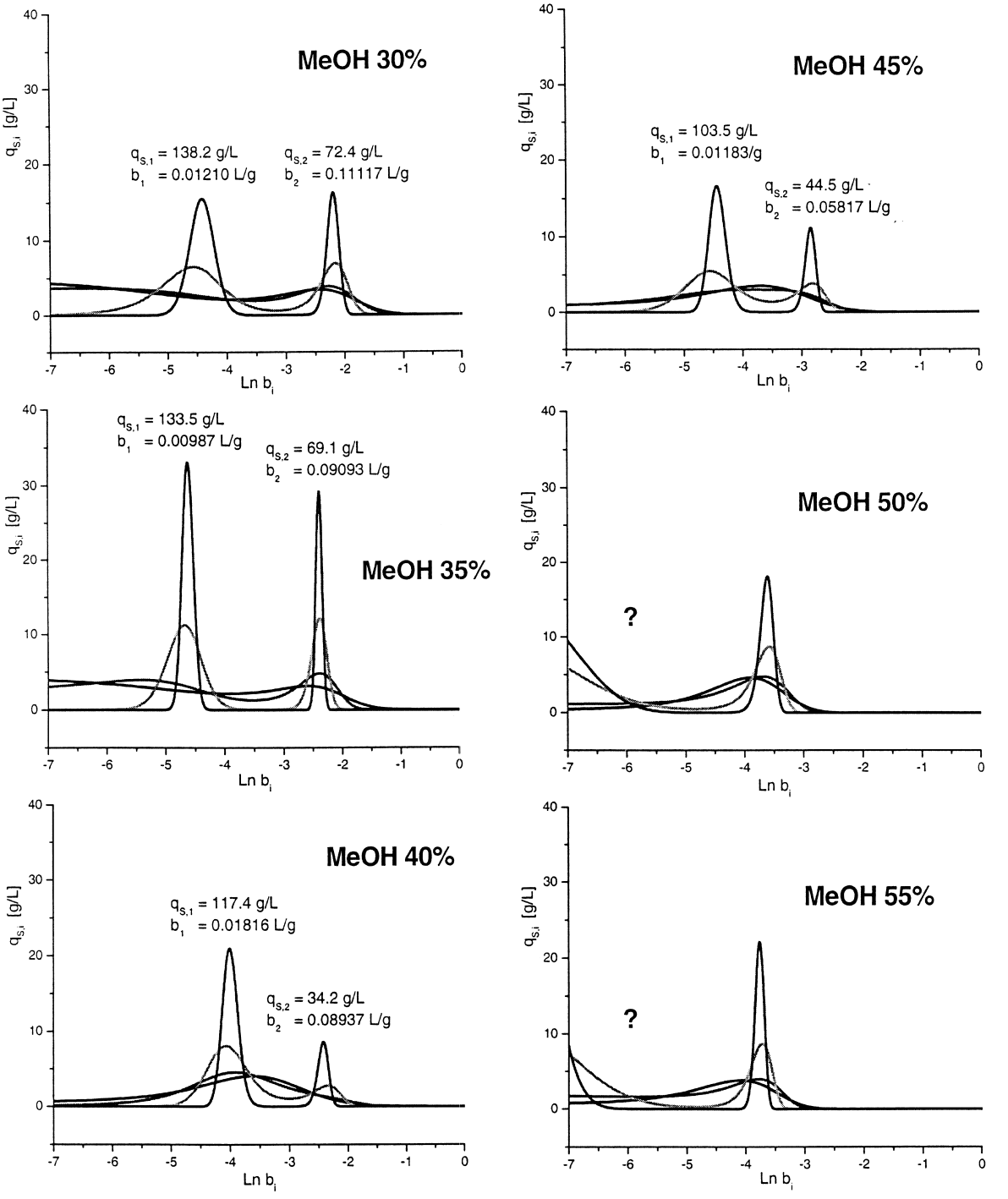

Fig. 6. Results of the calculation of the adsorption energy distribution functions of phenol using the expectation maximization procedure for the first series of FA runs. For each methanol–water composition, the four curves correspond to four different number of iterations input to the program (10^5, 10^6, 10^7 and 10^8 iterations). Note the difficulty encountered for the two highest methanol content (50 and 55%), where the procedure could not properly resolve the two energy bands.

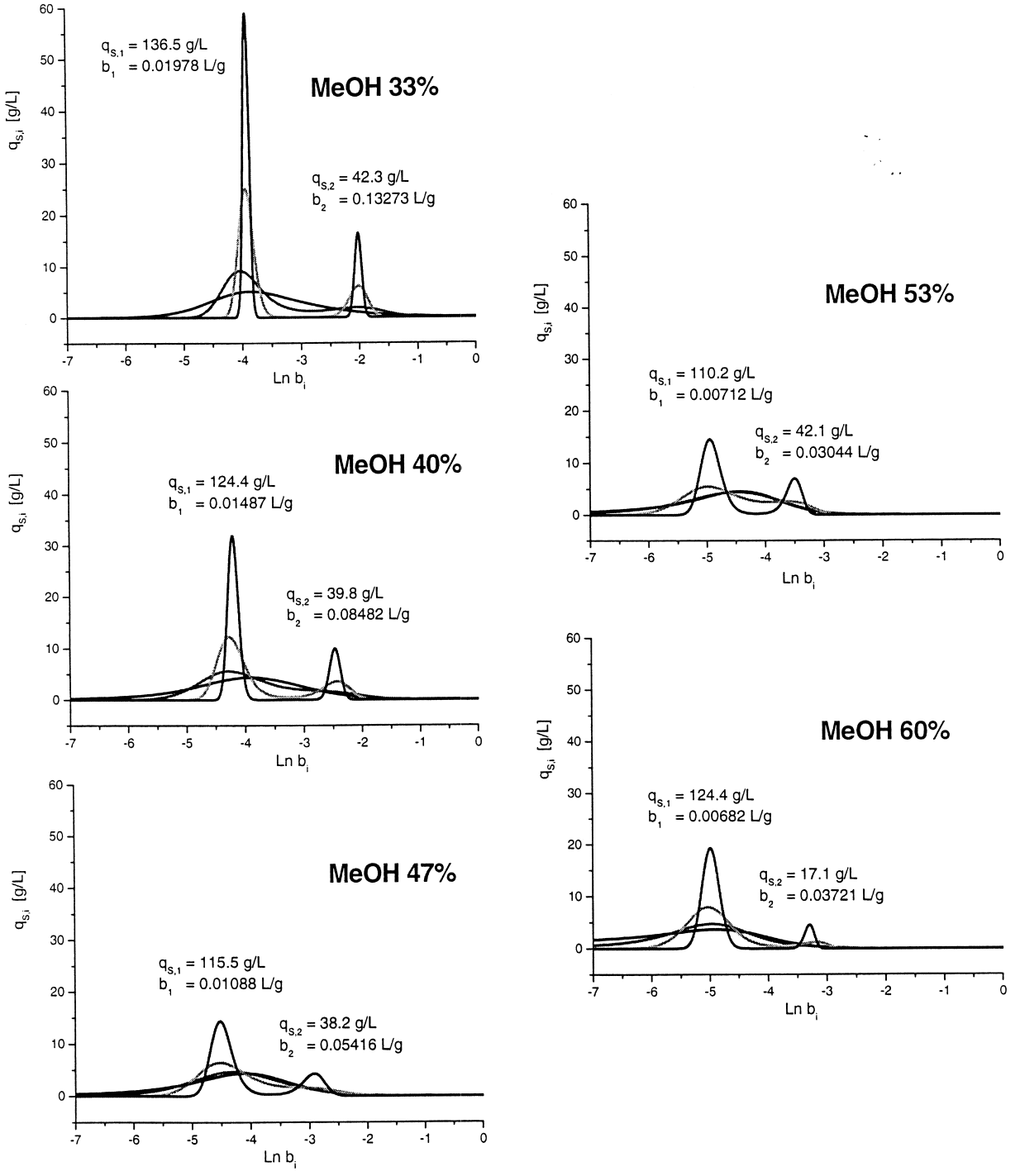

Fig. 7. Results of the calculation of the adsorption energy distribution functions of phenol using the expectation maximization procedure for the second series of FA runs. For each methanol–water composition, the four curves correspond to four different number of iterations input to the program (10^5, 10^6, 10^7 and 10^8 iterations). Note the complete resolution of the two energy bands at highest methanol content (53 and 60%) which were not resolved in Fig. 6 (see text).

versus 150 g/l at 45% and below. Numerous attempts (not shown) were made to improve the AEDs at the two highest methanol concentrations by changing the range of energy, the number of energy points, or the number of iterations in the calculations [31]. Their failure suggests that the low-energy part of the AED estimated by the program cannot be interpreted properly.

The only reasonable approach to determine the AED at high methanol concentrations was to extend the range of phenol concentrations within which the isotherm data were acquired. This was done in the second series of FA measurements for which methanol concentrations up to 100 g/l were used. The results confirmed this expectation since, despite a lower number of data points acquired, the EM method converged now toward the same expected bimodal distribution at high methanol concentrations (46.7, 53.3, and 60%) as it did at lower methanol concentrations (Fig. 7). Measurements were not carried out for methanol concentrations beyond 60% because, then, the retention factor becomes lower than 1 and, under such experimental conditions, data acquisition in FA becomes inaccurate. Then the precision of the isotherm parameters and of the AED derived from these measurements would become insufficiently precise.

The numerical values of the four parameters of the biLangmuir isotherm were derived from the fitting of the isotherm data to this model and from the results of the AED determinations made with the EM method, using the same experimental isotherm data. These two sets of parameters are compared in Fig. 8. The similarity of the various plots demonstrates the excellent agreement between the results of the two methods when applied to the same set of experimental data. The AED method predicts a slightly higher saturation capacity on the high-energy sites and, in partial compensation, a weakly lower saturation capacity on the low-energy sites (Fig. 8A and C). The two binding constants derived from the AED method are slightly larger than those derived from the fitting of the data to the model (Fig. 8B and D). The differences between the results of the two methods exhibit a barely significant trend to increase when the adsorption energy on the two types of sites becomes closer (i.e., around 50% methanol in the aqueous mobile phase). As can be seen in Fig. 7, the two energy bands are broader for the methanol concentrations of 47 and 53% than for lower (33 and 40%) or higher (60%) methanol concentrations. The elution band profiles of a large sample of phenol were calculated with the isotherms derived from the AED, under the same experimental conditions as in Fig. 3. The profiles obtained are nearly identical to those calculated with the biLangmuir isotherm derived earlier from the fitting of the experimental adsorption data to this model. They cannot be distinguished visually so they are not shown in the figure.

The contributions of the high- and low-energy types of sites to the retention factor (i.e., the product $Fq_{S,i}b_i$) are equal for a methanol concentration close to 50%. This is illustrated in Fig. 9 for the two series of isotherm data measurements. At high methanol concentrations, the low-energy sites control the retention factor at infinite dilution, through the interactions of phenol within the C_{18} chains. At low methanol concentrations, the retention of phenol is controlled by the high-energy sites, i.e., by the interactions of the phenol molecules and the accessible sites at the surface of the adsorbent where the C_{18} density is locally lower than on the major part of the bonded surface. Note that, while the results of the two series of measurements are consistent qualitatively, there are some significant differences between the two series of numerical values, probably because they were obtained for different ranges of methanol concentrations. Also the first series of FA measurements made at 40% methanol were probably affected by some systematic error.

4.5. Adsorption energies on the two different types of sites

The AEDs reported in this work are given as distributions of the adsorption constant, *b*. The advantage of this choice is that it does not require the knowledge of the preexponential factor in Eq. (3) for which, at this stage, we have no good estimate. If we assume that the preexponential factor is the same for all the sites on the surface of the stationary phase, an assumption which is generally made in adsorption studies [17,20,22,23], we can calculate the difference between the mean adsorption energies on the two type of sites. It is given by the following equation:

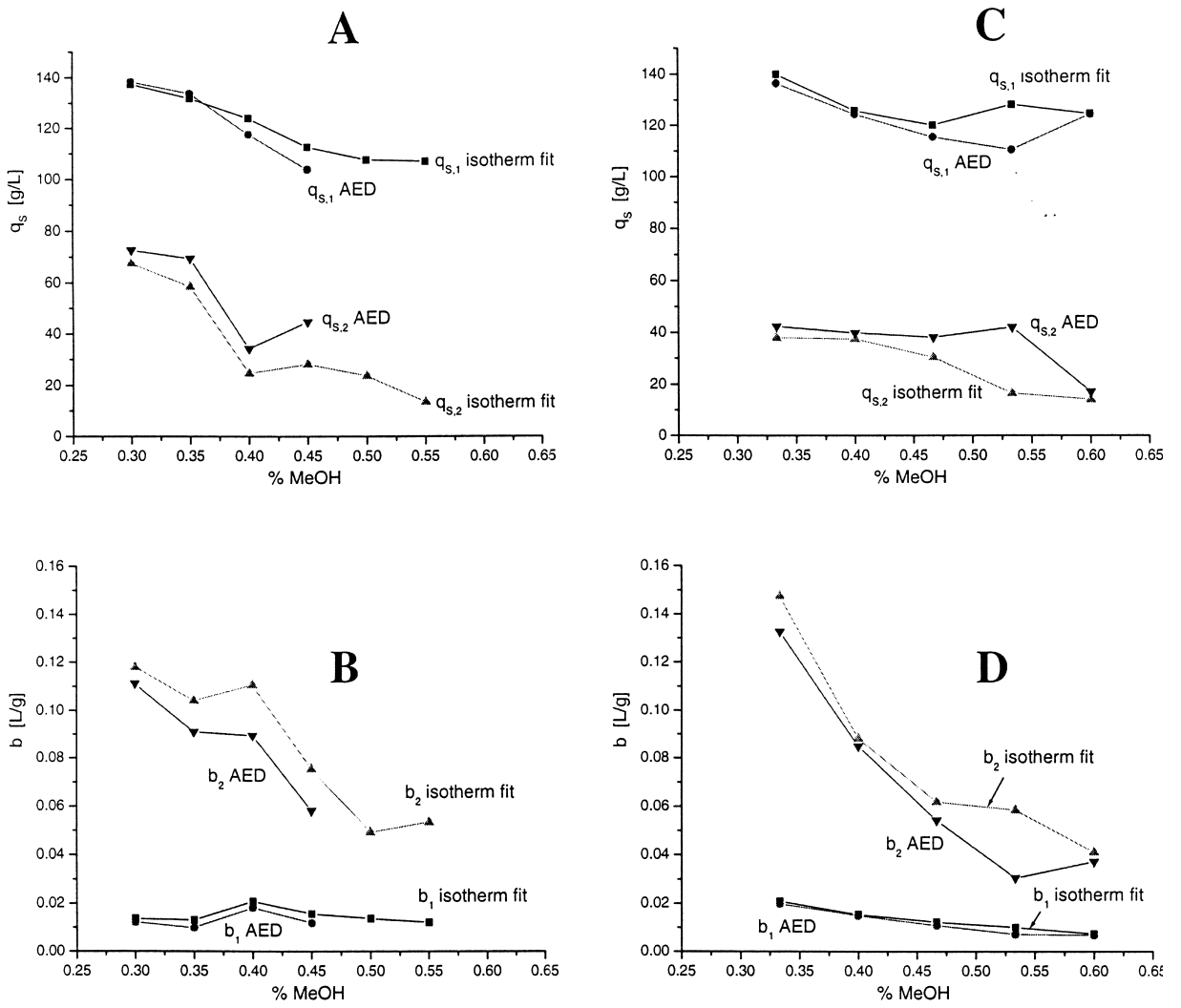

Fig. 8. Comparison between the results of the regression analysis (Fig. 5) and those of the AED approach of the experimental adsorption data of phenol on the C_{18}-Kromasil column. Left (A and B, $C_{max}=50$ g/l) and right (C and D, $C_{max}=100$ g/l) series of FA runs. Top (A and B), saturation capacities. Bottom (C and D), adsorption constants. Note that the AED approach overestimates the saturation capacities and underestimates the binding constants compared to the regression analysis results.

$$\varepsilon_{a,2} - \varepsilon_{a,1} = RT \ln\left(\frac{b_2}{b_1}\right) \quad (16)$$

The values of $\Delta\varepsilon = \varepsilon_{a,2} - \varepsilon_{a,1}$ are plotted in Fig. 10 versus the methanol concentration in the mobile phase. This difference is nearly constant and close to 4 kJ/mol at methanol concentrations above 40%, it is possibly slightly higher at low methanol concentrations. It is slightly below $2RT$. This difference is of the order of magnitude expected for the difference of interaction energies between dispersive and polar interactions.

5. Conclusion

The influence of the mobile phase composition on the retention factor, i.e., on the initial slope of the isotherm has been known since the beginning of liquid chromatography. Our results demonstrate that

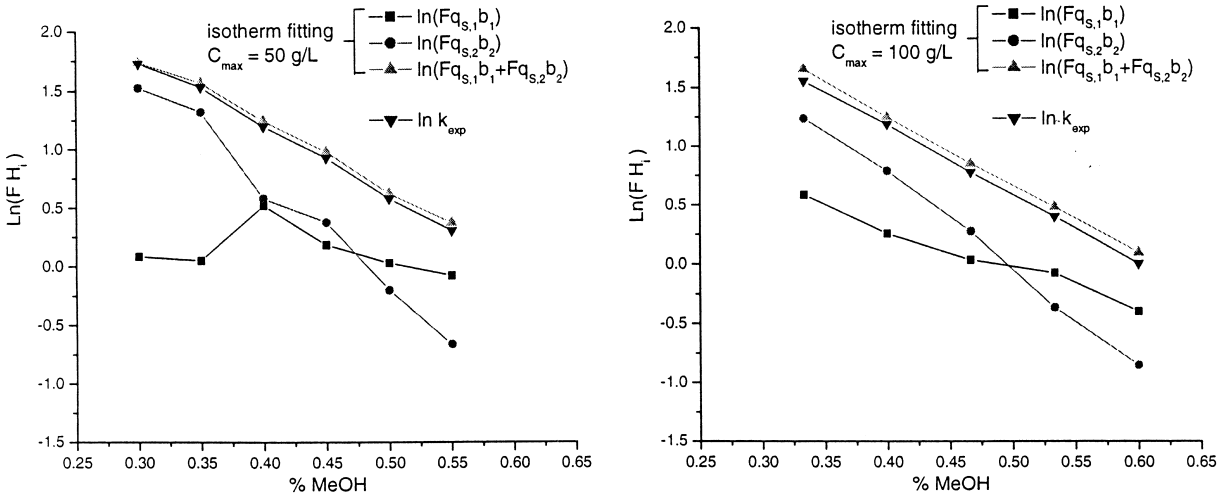

Fig. 9. Plots of the logarithm of the contribution of each type of sites i ($i = 1$ low-energy sites; $i = 2$ high-energy sites) to the retention of phenol $\ln(Fq_{S,i}b_i)$ on the C_{18}-Kromasil column as a function of the methanol concentration in the mobile phase.

this composition has an important effect on the numerical values of all the parameters of the adsorption isotherm, hence on the high concentration band profiles of phenol on at least one brand of C_{18}-bonded silica, Kromasil. It is highly probable that a similar result would be observed with most or all other C_{18}-bonded silica adsorbents and for numerous other compounds.

Although the numerical values of the parameters of the isotherm model vary with the composition of the mobile phase, the model that accounts best for the adsorption isotherm data remains the same over the whole range of methanol concentration studied (30 to 60%, v/v), the biLangmuir model. This suggests the presence of two different types of adsorption sites on the adsorbent surface. The parameters of the high-energy sites (which could correspond to electrostatic interactions with the free silica surface) are the more sensitive to changes of the mobile phase composition. Both their saturation capacity and the corresponding binding energy decrease by a factor of 3 when the methanol concentration increases from 30 to 60% methanol. Accordingly, the contribution of these high-energy sites to the adsorption of phenol decreases 10-fold. By contrast, the saturation capacity and the binding energy of the low-energy sites (arising probably from dispersive interactions between the solute and the bonded C_{18} chains) are less affected. The former decreases by less than 20% and the latter by a factor of 2. Thus, this work opens new vistas on the nature of the retention mechanism(s) on chemically bonded phases which might be more complex than assumed generally.

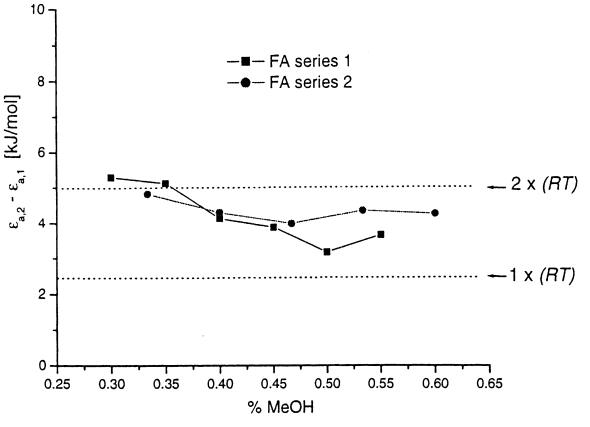

Fig. 10. Plot of the difference of adsorption energy between the high- and the low-energy sites versus the methanol concentration in the mobile phase.

From a practical viewpoint, it is important to know the dependence of the isotherm parameters on the mobile phase composition in order either to calculate the band profiles under overloaded gradient elution conditions or to determine the optimum experimental conditions for the isocratic preparative

separation of a mixture. The results reported here show that the variation of the saturation capacity with the eluent composition may be important. The influence of the mobile phase composition on the yield and the production rate achieved may be far more important than usually suspected, especially when small molecules are involved. It has been clearly demonstrated that performance in preparative chromatography is strongly affected by the saturation capacity of the phase system selected [1,3,31,32].

Acknowledgements

This work was supported in part by grant CHE-00-70548 of the National Science Foundation and by the cooperative agreement between the University of Tennessee and the Oak Ridge National Laboratory. We thank Hans Liliedahl and Lars Torstenson (Eka Nobel, Bohus, Sweden) for the generous gift of the columns used in this work and for fruitful discussions.

References

[1] G. Guiochon, S.G. Shirazi, A.M. Katti, Fundamentals of Preparative and Nonlinear Chromatography, Academic Press, Boston, MA, 1994.
[2] G. Guiochon, J. Chromatogr. A 965 (2002) 129.
[3] A. Felinger, G. Guiochon, J. Chromatogr. A 796 (1998) 59.
[4] D.M. Bliesner, K.B. Sentell, J. Chromatogr. 631 (1993) 23.
[5] D.M. Bliesner, K.B. Sentell, Anal. Chem. 65 (1993) 1819.
[6] J.L. Wysocki, K.B. Sentell, Anal. Chem. 70 (1998) 602.
[7] C.R. Yonker, T.A. Zwier, M.F. Burke, J. Chromatogr. 241 (1982) 257.
[8] C.R. Yonker, T.A. Zwier, M.F. Burke, J. Chromatogr. 241 (1982) 269.
[9] R.M. McCormick, B.L. Karger, Anal. Chem. 52 (1980) 2249.
[10] P. Jandera, Z. Posvec, P. Vraspir, J. Chromatogr. A 734 (1996) 125.
[11] P. Jandera, G. Guiochon, J. Chromatogr. 588 (1991) 1.
[12] Z. El Fallah, G. Guiochon, Anal. Chem. 63 (1991) 2244.
[13] F. Gritti, G. Gotmar, B.J. Stanley, G. Guiochon, J. Chromatogr. A 983 (2003) 51.
[14] G. Zhong, P. Sajonz, G. Guiochon, Ind. Eng. Chem. (Res.) 36 (1997) 506.
[15] H. Poppe, J. Chromatogr. A 656 (1993) 19.
[16] Z. Ma, A. Katti, B. Lin, G. Guiochon, J. Phys. Chem. 94 (1990) 6911.
[17] M. Jaroniec, R. Madey, Physical Adsorption on Heterogeneous Solids, Elsevier, Amsterdam, 1988.
[18] D. Graham, J. Phys. Chem. 57 (1953) 665.
[19] R.J. Umpleby II, S.C. Baxter, Y. Chen, R.N. Shah, K.D. Shimizu, Anal. Chem. 73 (2001) 4584.
[20] J. Toth, Adsorption, Marcel Dekker, New York, 2002.
[21] B.J. Stanley, S.E. Bialkowski, D.B. Marshall, Anal. Chem. 65 (1993) 259.
[22] D.M. Ruthven, Principles of Adsorption and Adsorption Processes, Wiley, New York, 1984.
[23] M. Suzuki, Adsorption Engineering, Elsevier, Amsterdam, 1990.
[24] P.W. Danckwerts, Chem. Eng. Sci. 2 (1953) 1.
[25] K. Kaczmarski, M. Mazzotti, G. Storti, M. Morbidelli, Comput. Chem. Eng. 21 (1997) 641.
[26] K. Kaczmarski, Comput. Chem. Eng. 20 (1996) 49.
[27] K. Kaczmarski, D. Antos, J. Chromatogr. A 862 (1999) 1.
[28] P.N. Brown, A.C. Hindmarsh, G.D. Byrne, procedure available from http://www.netlib.org.
[29] M. Kele, G. Guiochon, J. Chromatogr. A 855 (1999) 423.
[30] F. Gritti, G. Guiochon, J. Chromatogr. A (2003) in press.
[31] A. Felinger, G. Guiochon, AIChE J. 40 (1994) 594.
[32] A. Felinger, G. Guiochon, Biotechnol. Prog. 12 (1996) 638.